UTILIZATION OF ORBITAL ULTRASOUND AND OPTICAL COHERENCE TOMOGRAPHY IN PAPILLEDEMA AND PSEUDOPAPILLEDEMA PATIENTS

By

Roberto Saenz
O.D.

THESIS

In partial satisfaction of the requirements for the degree of

MASTER OF SCIENCE

in

PHYSIOLOGICAL OPTICS

Presented to the

Graduate Faculty of the

College of Optometry
University of Houston

August, 2016

Approved:

Han Cheng, O.D., Ph.D. (Chair)

Rosa Tang, M.D., M.P.H., M.B.A.

Laura Frishman, Ph.D.

Committee in Charge

Acknowledgements

I would like to thank Dr. Cheng for being such a great mentor. From the beginning, any of our classmates could tell that she teaches and thinks at a different level. Her ability to relate and teach so efficiently inspired me from the very beginning. I can't thank her enough for her patience, all the effort that she has contributed toward me, and for continually pushing me to get to the next level. I know that everything I have and will achieve in my career will trace back to these four years where Dr. Cheng's aided in establishing my foundational knowledge and thought processes.

I would also like to thank the other members of my committee, Dr. Frishman and Dr. Tang. First, I want to thank Dr. Frishman and all others, who played a role in allowing UHCO to have the combined O.D./M.S. degree. I would also like to thank the members of the summer research committee and NIH (T35 EY07088) for developing my interest in understanding why things happen. UHCO rivals any optometry school out there, when it comes to neuro-optometry, in that we are associated with a great neuro-ophthalmologist who loves to teach. From the very beginning, Dr. Tang has taken me in with open arms. I am thankful for all the meetings I was allowed to sit in on, all the patients I was allowed to sit it on, and all the cases I was allowed to go through in order to develop this research. I have enjoyed the relationship with Dr. Tang and the ability it allows UHCO to be a pioneer in neuro-ophthalmic relations.

I would like to thank Dr. Prager for his insight on orbital ultrasound, allowing me to observe his technique, and discuss the clinical applications. I would also like to thank Dr. Pass for all of his teaching and discussions on the topic of papilledema. His wealth of knowledge and methods of teaching were an inspiration. I also would like to thank Divya Narayanan for all her assistance in getting acclimated into the research lab. She spent

many hours explaining and re-explaining things to me in the early days and I am very grateful.

Foremost, I would like to thank my wife for all of her love and support in allowing me to complete this program. She has helped me in ways that would be longer than this thesis if I were to write them out. None of what I accomplish could be done without her. I would also like to thank my parents for their love and their encouragement through out the years.

Abstract

Purpose: To evaluate the use of two non-invasive and low-cost tests, orbital ultrasound and optical coherence tomography (OCT), in differentiating papilledema (PE) from pseudopapilledema (PPE).

Methods: Retrospective cross-sectional analysis included 51 patients referred to a neuro-ophthalmologist for presumed PE who were diagnosed with PE (n = 23, median Frisen scale II) or PPE (n = 28, 13 buried drusen and 15 obliquely inserted optic nerves) based on a thorough history, ocular/neurological exams and ancillary tests. Orbital ultrasound consisted of a B-scan to detect buried drusen and a standardized A-scan to measure optic nerve sheath diameter (ONSD). If ONSD at primary gaze exceeded normal limits (4.2 mm), a 30° test was performed to measure the ONSD at 30° lateral gaze. A Cirrus OCT Optic Disc Cube 200x200 scan was used to obtain the retinal nerve fiber layer thickness (RNFLT).

Results: The mean ONSD (mm) at primary gaze was larger in PE (5.4 ± 0.6) than PPE (4.0 ± 0.3, $p < 0.0001$). The percent change in the ONSD at 30° gaze was greater in PE (22.4 ± 8.4) than PPE (2.8 ± 4.8, $p < 0.0001$). Average RNFLT (μm), was thicker in PE (219.1 ± 104.6) than PPE (102.4 ± 20.1, $p< 0.0001$). ONSD and 30° test had the greatest area under the ROC curve (AUC), 0.98 and 0.97, respectively; followed by inferior quadrant (0.90) and average RNFLT (0.87). In a subgroup of mild PE (Frisen scale I-II, n = 15), AUC remained high for ONSD (0.95) and 30° test (0.93) but decreased to 0.71 for average RNFLT. At 95% specificity, sensitivity (%) for ONSD, 30° test and average RNFLT was 91.3, 91.3 and 56.5, respectively for the entire PE group; 80.0, 86.7 and 13.3 for the mild PE subgroup.

Conclusion: Orbital ultrasound and OCT are useful ancillary tests that can be done, along with a thorough examination, to effectively differentiate PE from PPE. Due to its easy access, RNFLT can potentially be used to detect moderate to severe PE. Ultrasound measurements may further assist eye care providers in differentiating mild PE from PPE when ophthalmoscopic findings are non-diagnostic.

Table of Contents

List of Tables

List of Figures

Chapter 1: Introduction

1. Background

Papilledema (PE), optic disc edema secondary to increased intracranial pressure (ICP), indicates potentially life-threatening conditions such as intracranial masses, cerebral venous thrombosis, cranial injuries, subarachnoid hemorrhages, meningitis, and idiopathic intracranial hypertension (IIH) that require urgent medical management (1). Clinical history and ophthalmological findings are vital for the correct diagnosis. Increased ICP within the optic nerve sheath causes axoplasmic flow stasis, resulting in edema of the axons within the optic nerve head (2, 3). PE typically presents bilaterally, but can be asymmetrical or even unilateral (1, 4, 5). Prolonged PE can lead to permanent and severe vision loss (6). On ophthalmoscopy, PE may exhibit signs such as optic nerve head elevation, blurred optic disc margins, venous congestions, hemorrhages, soft/hard exudates, and choroidal/retinal folds (7). While ophthalmoscopy is a routine clinical procedure to detect optic disc edema, its accuracy depends on the severity of PE and the expertise of the clinician. Subtle PE can be especially difficult to accurately diagnose; and may be easily confused with pseudopapilledema (PPE), a group of benign conditions mimicking disc edema including optic nerve head drusen, nasally elevated nerves or crowded hyperopic discs, due to the presence of overlapping ophthalmic signs (e.g. disc elevation and blurry margins) in both PPE and PE. Systemic and visual symptoms associated with increased ICP and PE such as headache, nausea, vomiting, pulsatile tinnitus, transient visual obscuration, or diplopia are not necessarily specific or present in patients with PPE; abnormal visual acuity, pupillary responses, color vision or visual field defects (other than enlarged blind spots) are uncommon in acute PE (1). On the other hand, patients with PPE may have unrelated headaches,

visual disturbances or visual field defects that further complicate a clinician's decision making (8, 9).

In order to avoid ordering a costly and sometimes invasive neurological work-up in patients with PPE (10), ancillary testing such as optical coherence tomography (OCT) (11), orbital ultrasound (12, 13), and fluorescein angiography (14) has been utilized to improve diagnostic accuracy. The goal of this thesis is to evaluate the diagnostic abilities of orbital ultrasound and OCT in PE and PPE patients.

2. PE

2.1 Pathophysiology

Ever since Türck and Coccius first described PE independently in 1853, many have theorized about the underlying pathophysiology (15). In the mid-1800s, Türck (1853) and Von Graefe (1860) thought that in patients with cerebral tumors, venous stasis of the cavernous sinus secondary to increased ICP would mechanically cause a stagnation of blood flow in retinal veins, resulting in optic disc edema (15, 16). In 1898, Deyl proposed that in PE, the central retinal vein, which pierces the subarachnoid space in its course, becomes occluded as pressure in the perioptic subarachnoid space increases, thus leading to hyperemia and edema of the optic nerve (17). Many contradictory theories, both mechanical and non-mechanical in nature, existed without experimental support. It was not until 1960's that Hayreh conducted a series of anatomical and physiological studies in human cadavers and rhesus monkeys to understand the mechanism of PE (18). In 1965, Hayreh investigated the role of central retinal vein compression by cauterizing the central retinal vein where it exists the optic nerve sheath in six rhesus monkeys (19, 20). The funduscopic examination in three of

the monkeys did not show any optic disc edema (group I), while the other three did show some hyperemia of the nerve (group II). Hayreh then artificially elevated the ICP using an inflatable balloon placed inside the cranium in two monkeys (one from each group). Increased ICP successfully induced bilateral optic disc edema in the monkey from group I. The group II monkey exhibited marked disc edema in the fellow non-cauterized eye but only segmental edema of the disc when the ICP was elevated. Upon histopathological examination of the group II monkey, it was discovered that a segment of the optic nerve had been accidently cauterized, causing optic atrophy in the region. The atrophied part of the optic nerve did not exhibit any edema when the ICP was increased. Thus Hayreh disproved the idea that compression of the central retinal vein plays a primary role in the pathogenesis of PE, a prevalent belief at the time, and learned that intact nerve fibers must be present in order for PE to occur.

Upon anatomical examination, Hayreh discovered that the subarachnoid space between the optic nerve and its sheath is largest immediately behind the globe and narrowest in the region of the optic canal (19). He also established that successful transmission of the increased intracranial cerebrospinal fluid (CSF) pressure to the optic nerve sheath is a pre-requisite for developing optic disc edema because cutting open the retrobulbar optic nerve sheath (sheath fenestration) in rhesus monkeys prevented the development of optic disc edema when the ICP was raised. Hayreh (1977a,b) documented the evolution of PE in rhesus monkeys using stereoscopic color fundus photography and fluorescein angiography (2, 21). On stereoscopic fundus photography the first notable finding was elevation (swelling) of the optic disc at the lower pole, followed by the superior disc, then the nasal disc, and lastly the temporal disc. The blurring of the optic disc margin was the next sign (observed after “appreciable amount of optic disc edema”), followed by hyperemia of the optic disc, and late vascular changes

including capillary dilation, microaneurysms, hemorrhages, and venous engorgement. According to Hayreh, stereoscopic fundus photography was much more sensitive in detecting early optic disc edema than fluorescein angiography, which detects the vascular changes occurring later in the process, confirming that vascular changes are secondary to optic disc swelling.

Tso and Hayreh also conducted a series of histopathological studies on rhesus monkeys to further understand the pathogenesis of PE (3). Initially, they used light microscopy studies to confirm that prominent axonal swelling in the optic disc surface and the anterior part of the prelaminar region was a major factor in PE and believed it to be responsible for the edema seen on ophthalmoscopy. They then used horseradish peroxidase, injected intravenously, to show blood vessel leakage at the posterior part of the nerve fiber layer, prelaminar and laminar cribrosa regions; they concluded that optic disc edema reflects a combination of axonal swelling and fluid leakage from the blood vessels. Lastly, Tso and Hayreh injected tritiated leucine intravitreously and observed via autoradiographs of the optic nerve head that stasis of the axoplasmic flow is primarily the cause of axonal swelling (22). Thus, Hayreh concluded that the pathogenesis of PE is primarily a mechanical phenomenon. The increased CSF pressure is first transmitted to the perioptic subarachnoid space causing axoplasmic flow stasis, which leads to swelling of the nerve fibers and therefore the optic disc edema. The swelling of the optic nerve head then secondarily compresses the venules, which results in vascular changes such as venous stasis and fluid leakage. Optic disc edema in the setting of increased ICP represents a combination of swollen axons and the extracellular fluid leakage from blood vessels in the region.

2.2 Frisen Scale

The modified Frisen scale uses the optic nerve appearance via ophthalmoscopy to assess the degree of PE (23, 24). The hallmark sign of grade I is a C-shaped halo that has a temporal gap, grade II shows a circumferential halo, grade III is obscuration of one or more segments of major blood vessels leaving the optic disc, grade IV is obscuration of a major blood vessel on the disc, and grade V is complete vessel obscuration. The Frisen scale is limited because it is an ordinal scale. Also, it is a subjective evaluation and grading of PE, which can significantly vary among individuals, thus objective evaluation of PE, such as OCT, may prove to be useful over time (24).

3. PPE

PPE is a benign optic nerve head elevation, which can be caused by small crowded hyperopic discs, obliquely inserted discs, and optic disc drusen.

3.1 Tilted Optic Disc and Obliquely Inserted Discs

Tiled optic discs and obliquely inserted optic discs can be mistaken for mild PE due to bilateral, segmental elevation of the optic nerve (25). Tilted optic discs occur in 0.4 to 3.5% of the general population (25) and are thought to be associated with an incomplete closure of the fetal fissure (26). Indistinct margins and elevation of the tilted optic disc are most commonly in the superotemporal quadrant of the optic disc (27, 28), whereas obliquely inserted nerves are most commonly elevated nasally. Patients with either of these conditions are usually asymptomatic, but if they present with a non-specific symptom of headache or visual disturbance further testing may be required to rule out mild PE.

3.2 Small Crowded Discs and Myelinated Optic Discs

The small cup to disc ratio, elevated appearance, and indistinct borders of the small, crowded optic discs, generally seen in hyperopic patients with a shorter axial length (29), attribute to the challenge in properly diagnosing PPE. Small, crowded optic discs are usually around 1.95 ± 0.33 mm in size (30), whereas normal optic disc size are 2.69 ± 0.70 mm (31). Circumferential, bilateral myelinated discs can imitate PE as well, as it presents as an elevated disc, with indistinct margins and obscured vessels. However, this is a rare occurrence, as only 0.6 to 1% of people have myelination of nerve fiber layer anterior to the lamina cribrosa, and only 0.8% of the time are these findings bilateral (32).

3.3 Optic nerve head drusen

Optic nerve head drusen, which has a prevalence of 3.4 to 24 per 1,000 population (33), are calcified acellular bodies, consisting of mucopolysaccharides, amino acids, DNA, RNA, and iron (34) located anterior to the lamina cribrosa (35). They are most often in the nasal portion of the optic nerve head (36). The pathogenesis of optic nerve head drusen is not fully understood at this time, but there are theories. Tso (1981) suggests that an initial alteration in axoplasmic flow leads to intracellular mitochondrial calcification (37). Next, axonal degeneration leads to the deposition of calcium, presumably from mitochondria, and the formation of drusen. Another theory suggests that the abnormal vasculature seen in patients with optic nerve head drusen, such as abnormal tortuosity, dilated veins, and retino-choroidal collaterals may contribute to the formation of drusen by excessive deposition of plasma proteins (38, 39). Others have suggested that a smaller scleral canal can cause axoplasmic stasis through optic nerve compression (40), but Floyd et al measured scleral canals using OCT and determined that scleral canal size is probably not a factor in the pathogenesis of optic nerve head drusen (41). Further investigation is required to fully understand its pathogenesis.

Optic nerve head drusen can have various presentations. Those visible on ophthalmoscopy are termed surface drusen, whereas drusen not visible on ophthalmoscopy are buried drusen. Optic nerve head drusen can cause optic nerve head elevation and indistinct margins mimicking PE. Optic nerve head drusen can present bilaterally (42, 43) or unilaterally (42), and they can be small or large, ranging from 5-1000μm (34, 37). Optic nerve head drusen are thought to be inherited in an irregular dominant fashion (44), and typically begin in the younger patients as a buried drusen (42). Longitudinal studies have shown that buried drusen can migrate forward to become surface drusen (45). Surface drusen are easier to classify as PPE upon stereoscopic examination, thus our study will only evaluate buried drusen.

The difficulty in differentiating between optic nerve head drusen and PE, besides the funduscopic similarities, occurs when drusen patients, who are usually asymptomatic, present with visual field defects (46, 47), transient visual obscurations (TVOs) (33), or decreased visual acuity (48). Visual fields defects, most commonly enlarged blind spots or arcuate defects, appear in the second decade of life (49) and can progress mildly with age (50). Although visual field defects occur in 25-71% of patients, severe field loss and decreased in visual acuity are rare but can occur (48). Vision loss and TVOs are attributed to permanent or transient compromise of the vascular integrity of the optic nerve head, caused by the compressive effects of drusen (51). Even though PE and PPE can present similarly, it is vital that clinicians diagnose drusen correctly to avoid unnecessary invasive testing; therefore, we will next discuss the role of a thorough history in differentiating PE and PPE.

4. Symptoms of Elevated ICP

Many patients with elevated ICP have idiopathic intracranial hypertension (IIH), a condition of high ICP without identifiable brain or CSF abnormalities. The incidence of IIH is 1 in 100,000 in the general population and rises to 19.3 per 100,000 in obese female of childbearing age (52). Studies on IIH allow us to evaluate the symptoms involved in elevated ICP.

4.1 Headaches

In IIH, headaches are the most common presenting symptom, occurring in 84-94% of patients (53, 54). The headaches typically occur daily, are diffuse and might be so severe in nature that they may awaken the patient during sleep or exist with nausea (55). Studies have found that headaches associated with IIH are not distinguishable from tension headaches (56) or migraine (57-59). Headaches as a non-specific sign can cause problems when they present in a patient with PPE. A recent study by Kovarik et al (2015) reported 25 of the 34 pediatric patients referred for suspected PE had headaches, and 26 of them were determined to have PPE (60).

4.2 TVOs

Transient visual obscurations are episodes of transient blurred or loss of vision. TVOs in PE typically occur for less than 30 seconds and may be associated with postural changes. As discussed above in optic nerve head drusen, transient ischemia of the optic nerve is thought to contribute to TVOs in both PE and PPE (51, 61). TVOs have been shown to be useful in distinguishing between PE and PPE, as the occurrence of TVOs in PE patients (68%) is greater than in PPE and controls(13, 53). However, patients could be confused by TVOs associated with PE versus those from other causes (e.g., dry eyes).

4.3 Pulsatile Tinnitus

Pulse synchronous tinnitus, described as a whooshing sound, occurs in 52-58% of patients with elevated ICP and is useful in diagnosing PE (53, 54). The pathophysiology is not fully understood, but some postulate that it is due to alterations in the cerebral vasculature. For example, a patient with elevated ICP secondary to a unilateral venous stenosis has increased blood flow through the contralateral sinus causing the patient to hear the pulsating, whooshing sound (62).

4.5 Other symptoms

Retrobulbar pain (44%), diplopia (38%), and visual loss have also been reported in patients with elevated ICP (63). The sixth cranial nerve becomes vulnerable to the effects of elevated ICP as it passes over the petrous portion of the temporal bone. Sixth nerve palsy, found in 10-20% of patients with elevated ICP, can cause horizontal diplopia(55). The optic nerve can also be affected if the ICP is not controlled causing vision loss secondary to atrophy of the optic nerve (6).

All disc elevations are not necessarily due to edematous nerves and all PPE patients are not asymptomatic, in fact many of the symptoms from elevated in ICP are common in PPE or controls, thus we will investigate the role of ancillary testing, specifically orbital ultrasound and OCT, in differentiating PE and PPE.

5. Orbital Ultrasound

Orbital ultrasound helps diagnose PE by measuring the optic nerve sheath diameter (ONSD), which enlarges with elevated ICP. In recent years, neuro-intensive care providers have used B scans due to their relative ease of use, to measure the

ONSD and they have reported correlation between the enlarged ONSD and the increased ICP in patients with invasive ICP monitoring (64-66). Human postmortem and in vivo studies have shown that the retro-bulbar part of the optic nerve sheath, being surrounded by orbital fat only, expands quickly in response to CSF pressure elevation transmitted from the intracranial subarachnoid space (67, 68). Interestingly, in the field of ophthalmic ultrasonography, the recognized technique for detecting fluid around the retro-bulbar optic nerve is based on standardized A-scan procedures. In the early 1970s, Dr. Ossoinig first described standardized echography, which incorporates a special S-shaped amplifier and a calibration for tissue sensitivity, and stated that the most accurate means to measure ONSD with ultrasound is to use standardized A-scan (69, 70). He also introduced the 30° test to differentiate an enlarged ONSD secondary to increased subarachnoid CSF from other solid or infiltrative optic nerve lesions such as meningioma or glioma. When an enlarged ONSD is encountered, the 30° test is performed by comparing the A-scan measured ONSD at primary gaze to that at 30° lateral gaze. A reduction in the widening of the ONSD at lateral gaze is presumed to occur due to redistribution of the increased amount of CSF over a greater area. In the presence of a large amount of fluid, a 25% to 30% reduction in ONSD has been observed (71, 72).

The A-scan has been shown to be useful in differentiating between PE and PPE in children (12) and adults (13). Using A-scan, sensitivity has ranged from 85-90% and the specificity has ranged from 63-79%. The problem with A-scan to measure ONSD and perform the 30° test is that the technique requires extensive training and experience from the examiner. It is estimated that there are only around 150 trained orbital ultrasonagraphers in the USA (13).

Another use of orbital ultrasound is to detect optic nerve head drusen. Buried drusen are not detectable by ophthalmoscopy alone (43); however, they do contain

calcium, which is highly reflective upon autoflourescence, B-scan and CT scan imaging (40, 71, 73, 74). Of these three tests, B-scan is considered the most reliable in diagnosing buried drusen (75).

6. OCT

Ocular imaging over the past several years has increased in significance in diagnosing ocular diseases. Optical coherence tomography has emerged in many optometric/ophthalmologic practices because of its easy and quick use. Specifically, the high definition spectral domain (SD) OCT has allowed the optic nerve head to be analyzed both qualitatively and quantitatively, and has been utilized in differentiating between PE and PPE.

6.1 PE

Quantitatively, OCT has been used to demonstrate increased retinal nerve fiber layer (RNFL) thickness (RNFLT) in acute PE (11, 76-79), however, RNFL thinning occurs in chronic PE (80). A few studies have reported that the nasal quadrant may be the most useful in differentiating between PE and buried drusen (77, 79). Drusen most commonly occur in the nasal quadrant (36, 38) and can cause atrophy of RNFL nasally (78). In PE, the nasal RNFLT is thickened (11, 76, 78, 79), therefore, this quadrant may prove to have the greatest diagnostic value. Papillary elevation, another quantitative measure, was shown by Flores et al to be useful in distinguishing between PE and PPE (78).

There are other OCT measurements that have been assessed in detecting PE. For example, Kupersmith et al evaluated the retinal pigment epithelium (RPE)/Bruch's

membrane angulation with OCT, and found an inward angulation toward the vitreous in 67% of PE patients (81). Other measurements such as peripapillary total retinal thickness (TRT) have been studied. Several studies have shown that measuring TRT has a role in assessing severe PE, as it may have less machine algorithm failure in segmentation (24, 82). At this point it is not certain whether TRT will aid in differentiating subtle PE from PPE. Vartin et al concluded that TRT may help to increase the sensitivity to mild PE (83), but Bassi et al found that the average RNFLT and individual quadrant measurements (AUC = 0.63 - 0.79) performed slightly better than TRT (0.58 -0.60) in diagnosing PE (11). Two studies that have looked at both quantitative and qualitative OCT measurements in PE proved quantitative measures to have a greater diagnostic ability (76, 78). However, the difficulty in analyzing most of the studies that utilize OCT in differentiating PE and PPE, is that many authors have included optic neuritis and ischemic optic neuropathies in their optic disc edema groups, thus the results are not truly representative of the true PE population. To our knowledge there are only two studies that have evaluated the use of SD-OCT in differentiating between PE and PPE (11, 84). Bassi and Mohana found OCT to be useful (11), whereas a smaller study by Kulkarni et al (84), evaluating mild PE only, suggested that OCT was not reliable. Our study will seek to confirm if the quantitative measurements of OCT, such as RNFLT, are useful in detecting PE.

6.2 PPE

Savini et al (2006) and Johnson et al (2009) suggested the use of the OCT qualitatively to observe the subhyaloid hyporeflective spaces, paying particular attention to the internal contour of the optic nerve (76, 85). They used the terms ‘lumpy bumby’, to describe optic nerve head drusen, or ‘lazy V’, to describe PE. Lee et al (2011) proposed that high definition SD-OCT also allows the visualization of optic nerve head

drusen as hyperreflective papillary subretinal focal masses (77). Bassi and Mohana found that 100% of eyes with optic nerve head drusen (n = 19) showed a hyperreflective mass (11).

However, recent evidence suggested that optic nerve head drusen have a variety of presentations, depending on their size and location, and the age of the patient (86). It is difficult to diagnose optic nerve head drusen based on OCT alone, as the disc drusen can present as hyperreflective masses (77), hyporefelctive masses (87), increased RNFLT (86), decreased RNFLT (78), or even as normal in children (11). Interestingly, with the advent of enhanced depth imaging (EDI) OCT and swept source (SS) OCT, the ability to detect optic nerve head drusen may improve (88-90).

For small crowded discs versus mild PE, OCT was unable to accurately differentiate between the two (91), but for tilted optic discs OCT may prove to be useful as tilted optic discs show a decrease in RNFLT (27) whereas mild PE may show an increase.

7. The Current Study

Previous studies have examined the role of OCT RNFL thickness or A-scan 30° test individually in differentiating PE and PPE (11-13, 84). Although each technique is shown to be useful, there is variable sensitivity (63 to 77% for OCT, 85 to 90% for ultrasound) and specificity (55 to 71% for OCT, and 63 to 79% for ultrasound) across studies. It is also important to note that performing the 30° test with A scan requires great expertise whereas OCT is more easily done, and accessible in many clinics. Comparing the diagnostic performance of OCT and A-scan in PE and PPE in the same patients would allow us to understand the strengths and limitations of each technique,

and help us establish a diagnostic protocol. In our neuro-ophthalmology clinic, all patients with suspected PE or PPE underwent ultrasound evaluation by an examiner with over 30 years of experience in ophthalmic ultrasound techniques. To our knowledge, the present study is the first to include both SD-OCT and standardized A-scan on the same patients.

The aim of the current study was to evaluate and compare the utilization of orbital ultrasound and SD-OCT in differentiating PE and PPE patients. Specifically, the diagnostic performance of RNFLT, ONSD, and 30° test were examined. Although it is not expected to be useful for differential diagnosis, the macular ganglion cell inner plexiform (GCIP) thickness was included to evaluate retinal ganglion cell damage in PE and PPE patients.

Chapter 2: Methods

Subjects

A retrospective review of medical records from 2013 through 2015 from the University of Houston College of Optometry MS Eye CARE Clinic identified 23 subjects (mean age: 29.9 ± 11.0 years) with a definitive diagnosis of PE and 28 subjects (mean age 28.6 ± 11.8 years) with PPE, all referred for presumed PE. All patients underwent at least an initial comprehensive neuro-ophthalmologic examination that included dilated fundus examination by an experienced neuro-ophthalmologist, OCT, and an ultrasound evaluation of the optic nerve. Depending on the suspected etiology, further diagnostic work up might have included neurological evaluation with brain/orbital imaging, lumbar puncture, and other necessary tests (1, 10). In the PE group, all 23 subjects were diagnosed with IIH.[1] In the PPE group, 13 subjects showed buried optic disc drusen on B-scan and 15 subjects showed nasal elevation due to oblique insertion of the optic disc. Patients with a previous history of PE or those with ocular or systemic conditions that could potentially influence OCT/ONSD measurements were excluded.

Orbital Ultrasound

All ultrasound examination was performed by a very experienced examiner with the Aviso S system (Quantel Medical). B scan (10 MHz probe) was initially used to rule out buried optic nerve head drusen. Standardized A scan was used to measure the ONSD as described by Ossoinig and his colleagues (69, 70); the largest measurement with repeated measures was recorded. The A-scan seen in Figure 1 shows the initial probe spike (IP), followed by an area of minimal to no spikes, as sound travels through the vitreous (V), followed by the large spikes of the optic nerve sheath (S_1 and S_2). The

spikes from the sheath should be equal in amplitude and should have no major spikes in between them. If ONSD exceeded the lab-established normal limit (4.2 mm), the 30° test was performed. The reduction in ONSD measured at 30° lateral gaze compared to that at primary gaze was calculated as a percentage. A greater than 20% decrease in sheath diameter was considered a positive 30° test by our ultrasonagrapher. Figure 1 shows an example of the ONSD decreasing from the primary gaze (A) to the 30° gaze (B), presumably due to redistribution of the increased subarachnoid fluid over a larger area in PE.

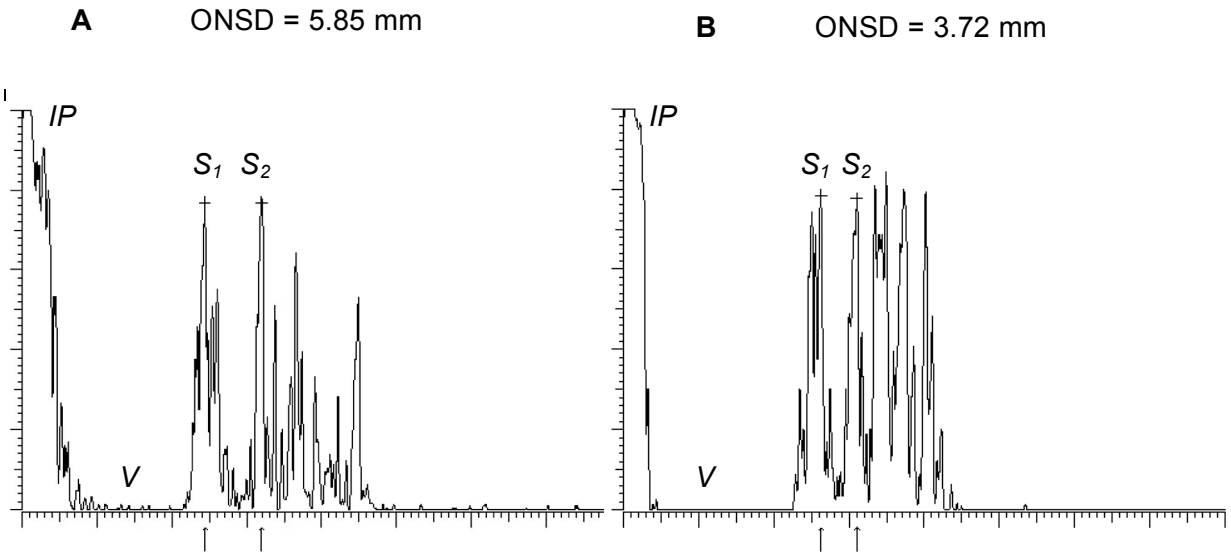

Figure 1. The A-scan shows the initial probe spike (IP), followed by an area of no spikes, as sound travels through the vitreous (V), followed by the optic nerve sheath (S_1 and S_2). The spikes from the sheath should be equal in amplitude and should have no major spikes in between them. An example of ONSD decreasing from the primary gaze (A) to the 30^o gaze (B), presumably due to redistribution of increased subarachnoid fluid over a larger area.

OCT

OCT was performed using Cirrus-HD OCT 4000 version 6.5 (Carl Zeiss Meditec Inc, Dublin, CA) by a trained ophthalmic technician. The average (avg) and quadrant peripapillary RNFLT data were obtained using the Optic Disc Cube 200 × 200 protocol that images the optic disc in a 6 mm x 6 mm area centered on the optic nerve. The average macular ganglion cell inner plexiform layer thickness (GCIPT) data were obtained using the Macular Cube 512 × 128 protocol that images a 6 mm × 6 mm area centered at the fovea. The machine software derived the GCIPT automatically for an elliptical annulus (2 mm × 2.4 mm radius), that excluded the central foveal region (0.5 mm × 0.6 mm radius). All OCT images had signal strength ≥ 7 and good centration, and were inspected for segmentation errors. Of the 23 PE patients, macular scans in 6 patients (both eyes in 3 of them, and the worse eye in the other 3 patients) showed erroneous segmentation for GCIPT upon visual inspection and were excluded (Figure 2). The avg or quadrant RNFLT and avg GCIPT were considered abnormally thickened when their values exceeded 95% of the age-matched machine normative database.

Statistics

Statistical analyses were performed using STATA 14.1 (StataCorp LP, College station, TX). For each subject, the eye with thicker RNFLT was selected for statistical analysis. Two-sample t-test was used to compare the means of various OCT and orbital ultrasound measures between the PE and PPE groups. Two proportion z-test was used to compare the percentages. The relationship between different variables, for example, RNFLT vs ONSD, RNFLT vs ICP for patients with PE was evaluated using Spearman Rho. Receiver operating characteristic (ROC) curves were constructed in Sigmaplot 10.0 (Systat Software, Inc) to evaluate the diagnostic performances of OCT and ONSD parameters. P values less than 0.05 were considered statistically significant.

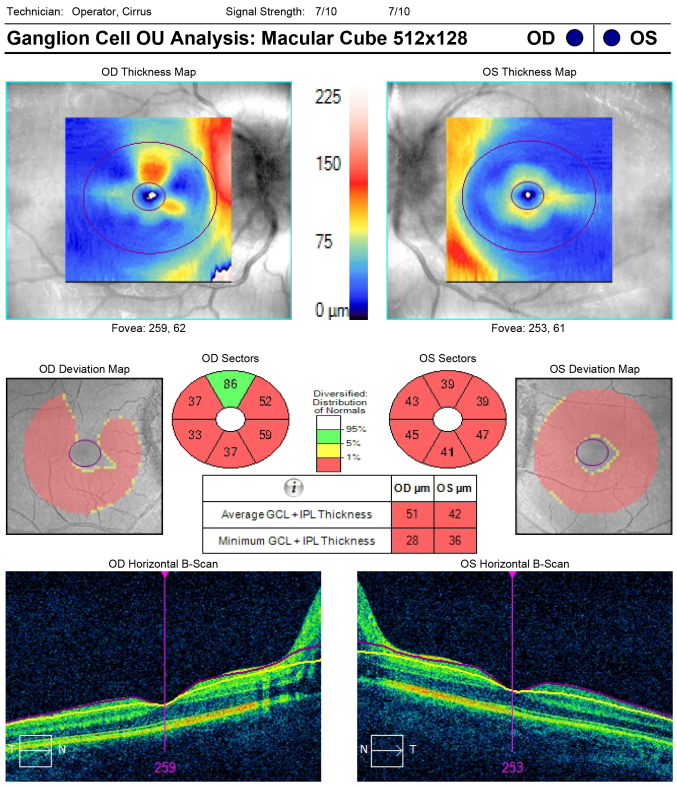

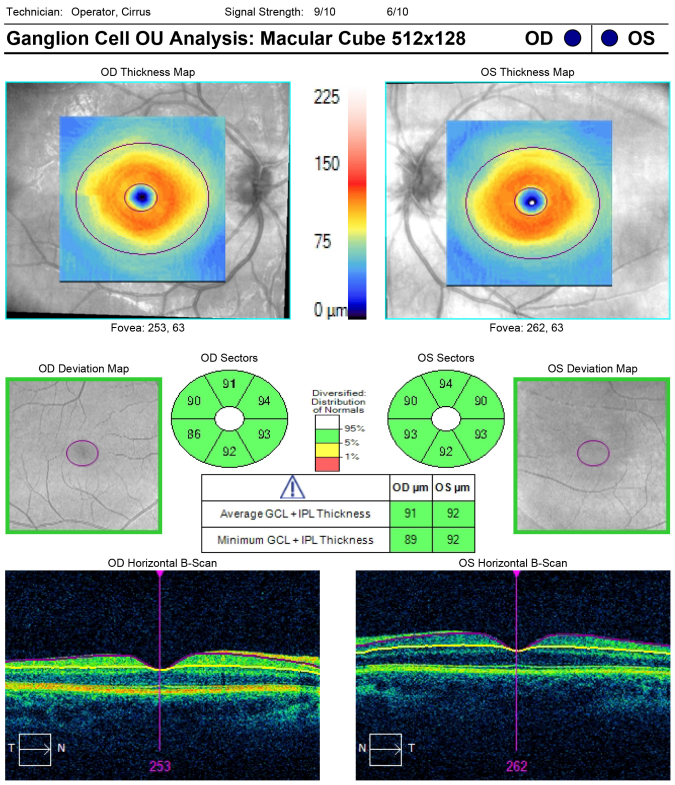

Figure 2. GCIPT in a patient with PE was artificially thin due to inadequate segmentation (left panel). GCIPT in the same patient measured 6 months later after PE subsided (right panel) was in the normal limits (82.1 ± 6.2 µm, Mwanza et al 2011) (92).

Chapter 3: Results

Patients' clinical characteristics

Table 1 summarizes patient characteristics for PE and PPE groups. Of the 51 patients referred in for presumed PE, 23 were diagnosed with PE (median Frisen scale 2) and 28 with PPE (13 buried drusen and 15 nasally tilted nerves). The mean age was similar between PE (29.9 ± 11.0) and PPE groups (28.6 ± 11.8, p = 0.69). There were more females than males in the PE group (21: 2) than the PPE group (14:14) (p = 0.0016), as well as a greater number of obese individuals (BMI > 30) in the PE group (78%) than the PPE group (25%) (p = 0.0002). The most common symptoms in the PE group were headache (91%), transient visual obscurations (61%), and tinnitus (35%). All PPE patients had at least one symptom; with the most common being headache (86%), followed by transient visual obscurations (57%) and tinnitus (21%). There were no statistical differences in the prevalence of the above-mentioned symptoms between the two groups.

Table 1: Comparison of demographic and clinical characteristics

	Papilledema (n = 23)	**Pseudopapilledema (n = 28)**
Age (years)*	29.9±11.0	28.6±11.8
F:M	21:2	14:14
Obese (BMI>30)	18 (78%)	7 (25%)
LP OP (cmH_20)*	31.0±9.9	NA
Buried drusen	NA	13 (46%)
Nasally tilted	NA	15 (54%)
Frisen scale (n) †	I (3), II (9), III (5), IV (6)	
Symptoms		
Headache	21 (91%)	24 (86%)
TVO	14 (61%)	16 (57%)
Tinnitus	8 (35%)	6 (21%)
Double vision	1 (4%)	0 (0%)
Eye pain	1 (4%)	1 (4%)
VA 20/20 or better	23 (100%)	27 (96%)

*mean ± SD; †based on the worse eye in asymmetrical PE cases;

LP OP: lumbar puncture opening pressure; TVO: transient visual obscuration

Comparing ultrasound and OCT measurements between PE and PPE

The mean ONSD (mm) at primary gaze was larger in PE (5.4 ± 0.6) when compared to PPE (4.0 ± 0.3, $p < 0.0001$) (Table 2). On the 30° test, a larger percentage of reduction in ONSD was observed in the PE group (22.4% ± 8.4) than in the PPE (2.8% ± 4.8, $p < 0.0001$).

The mean avg RNFLT (μm) was increased in PE (219.1 ± 104.6) when compared to PPE (102.4 ± 20.1, $p < 0.00001$ for all) (Table 2). The respective quadrant RNFLT for PE and PPE was 277.7 and 122.9 superiorly, 173.6 and 80.4 nasally, 281.0 and 136.8 inferiorly, and 121.3 and 66.1 temporally. Six PE eyes (26%) had the GCIP inaccurately segmented by the machine algorithm causing an artificially thin GCIP layer thickness despite strong signal strength. After excluding the inaccurately segmented PE eyes, GCIP thickness (μm) was slightly decreased in PPE (80.9 ± 13.1) when compared to PE (86.0 ± 5.5, $p < .04$).

Compared to age-matched machine norms, more PE eyes (56.5% to 87.0%) showed abnormal RNFL thickening than PPE eyes (14.3% to 25.0%). The inferior quadrant showed the greatest percentage (87.0%) followed by the avg RNFLT and superior quadrant (69.6% for both).

Table 2: Comparisons of ultrasound findings and OCT findings for PE and PPE

	Papilledema (n = 23)	**Pseudopapilledema (n = 28)**	**p**
ONSD (mm) at primary gaze	5.4±0.6	4.0±0.3	< 0.0001
ONSD change at 30° gaze (%)	22.4±8.4	2.8±4.8	< 0.0001
% (+) with >10%*	91.3	14.3	
% (+) with >13.5%†	91.3	3.57	
% (+) with >20%‡	82.6	0.00	
Avg RNFLT (μm)	219.1±104.6	102.4±20.1	< 0.0001
range (μm)	102-426	60-168	
% thickened§	69.6	25.0	0.001
Superior RNFLT	277.7±158.7	122.9±31.3	< 0.0001
% thickened§	69.6	14.3	0.001
Nasal RNFLT	173.6±101.4	80.4±37.4	0.0001
% thickened§	65.2	17.9	0.0006
Inferior RNFLT	281.0±146.5	136.8±29.7	<0.0001
% thickened§	87.0	21.4	<0.0001
Temporal RNFLT	121.3±63.6	66.1±13.2	<0.0001
% thickened§	56.5	14.3	0.001
GCIPT (μm)	86.0±5.5	80.9±13.1	0.04
% inaccurately segmented	26.1	0.0	

*a commonly suggested criterion (71); †based on ROC analysis (Table 3); ‡based on our ultrasonagrapher's experience; §thicker than the age-matched machine norms; ONSD: optic nerve sheath diameter

Receiver Operating Characteristic (ROC) analysis

In Figure 3, each ROC curve was constructed by plotting *Sensitivity* (the true positive rate where PE eyes were correctly classified) against *1 – Specificity* (the false positive rate where PPE eyes were misclassified as PE) when the parameter's threshold value was varied. Of all the ultrasound and OCT measurements, the ONSD and the 30° test had the greatest area under the curve (AUC), 0.98 and 0.97, respectively; followed by the inferior quadrant (0.90), and the avg RNFLT (0.87) ($p < 0.0001$ for all) (Table 3). The AUCs for the ONSD and the 30° test were significantly different from that of the avg RNFLT ($p = 0.013$ and 0.015, respectively), but did not reach statistical difference when compared to that of the inferior RNFLT ($p = 0.05$ and 0.08, respectively). The ONSD and the 30° test showed the same sensitivity (91.3%) and specificity (96.4%) with a cutoff value of 4.59 mm and 13.50%, respectively. At 96.4% specificity, the sensitivity was 56.5%, 52.2%, 69.6%, 43.5% and 56.5% for the avg, inferior, superior, nasal and temporal RNFLT, respectively. The GCIP showed no diagnostic value in differentiating between PE and PPE (AUC = 0.6429, $p = 0.114$).

Table 3: Diagnostic performance for ultrasound and OCT in differentiating PE from PPE

	AUC (95% CI)	**Cutoff value**	**Sensitivity%* (95% CI)**	**LR+**	**LR-**
ONSD	0.98 (0.95-1.00)	4.59 mm	91.3 (72.0-98.9)	25.6	0.09
30^{o} test	0.97 (0.94-1.01)	13.50%	91.3 (72.0-98.9)	25.6	0.09
Avg RNFLT	0.87 (0.77-0.96)	156.0 μm	56.5 (34.5-76.8)	2.1	0.29
S	0.83 (0.71-0.95)	163.5 μm	69.6 (47.1-86.8)	9.7	0.33
N	0.83 (0.71-0.95)	197.0 μm	43.5 (23.2-65.5)	4.1	0.3
I	0.90 (0.82-0.98)	213.5 μm	52.2 (30.6 - 73.2)	3.9	0.2
T	0.84 (0.73-0.96)	93.5 μm	56.5 (34.5 - 76.8)	4.4	0.2

*For all measurements, specificity (95% CI) was set to 96.4% (81.7%-99.9%).

PE: papilledema; PPE: pseudopapilledema; AUC: area under the ROC curve; ONSD: optic nerve sheath diameter; S, N, I, T: superior, nasal, inferior, and temporal quadrant RNFLT; LR+: positive likelihood ratio, LR-: negative likelihood ratio.

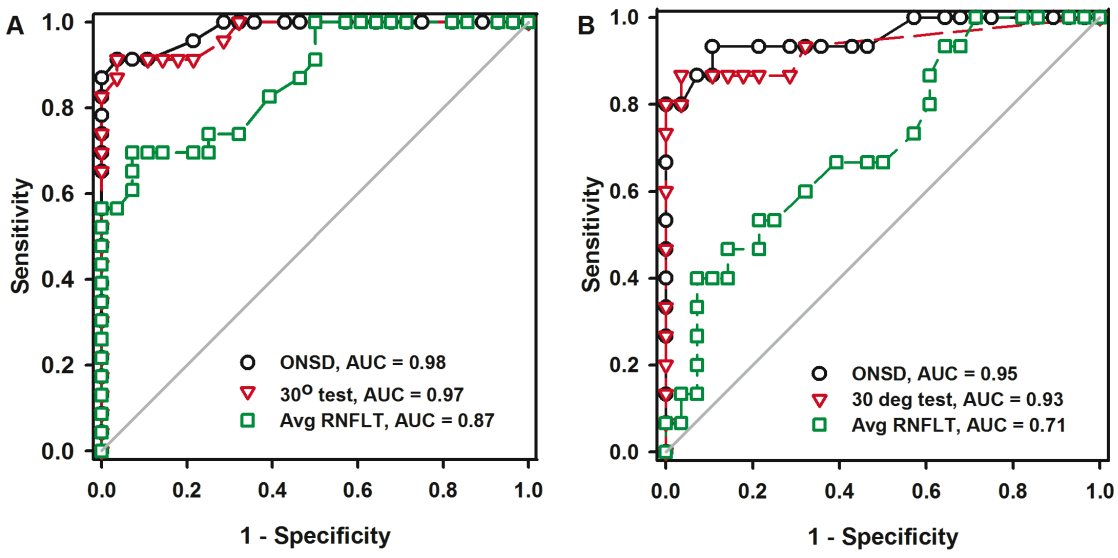

Figure 3. ROC curve for ONSD, 30° test and avg RNFLT in differentiating (A) all PE eyes (Frisen I to IV) and (B) mild PE eyes (Frisen I & II) from PPE.

Relationship between various measurements in PE

Spearman's Rho (rho) was used to assess the correlation between the lumbar puncture (LP) opening pressure and various ultrasound and OCT measurements (Figure 4). There was no observable correlation between LP opening pressure and ONSD (rho = 0.01, p = 0.95), 30° test (rho = 0.22, p = 0.31), or avg RNFLT (r = 0.17, p = 0.44), (Figure 4A-C). However, significant correlation was seen between LP opening pressure and the Frisen scale (rho = 0.48, p = 0.019) (Figure 4D).

Positive correlation was seen between the avg RNFLT and ONSD (rho = 0.49, p = 0.018) (Figure 5A), but not between avg RNFLT and 30° test (rho = 0.14, p = 0.54) (Figure 5B). Frisen scale grading correlated with both ONSD (rho = 0.52, p = 0.011) (Figure 5C) and avg RNFLT (rho = 0.70, p = 0.0002) (Figure 5D).

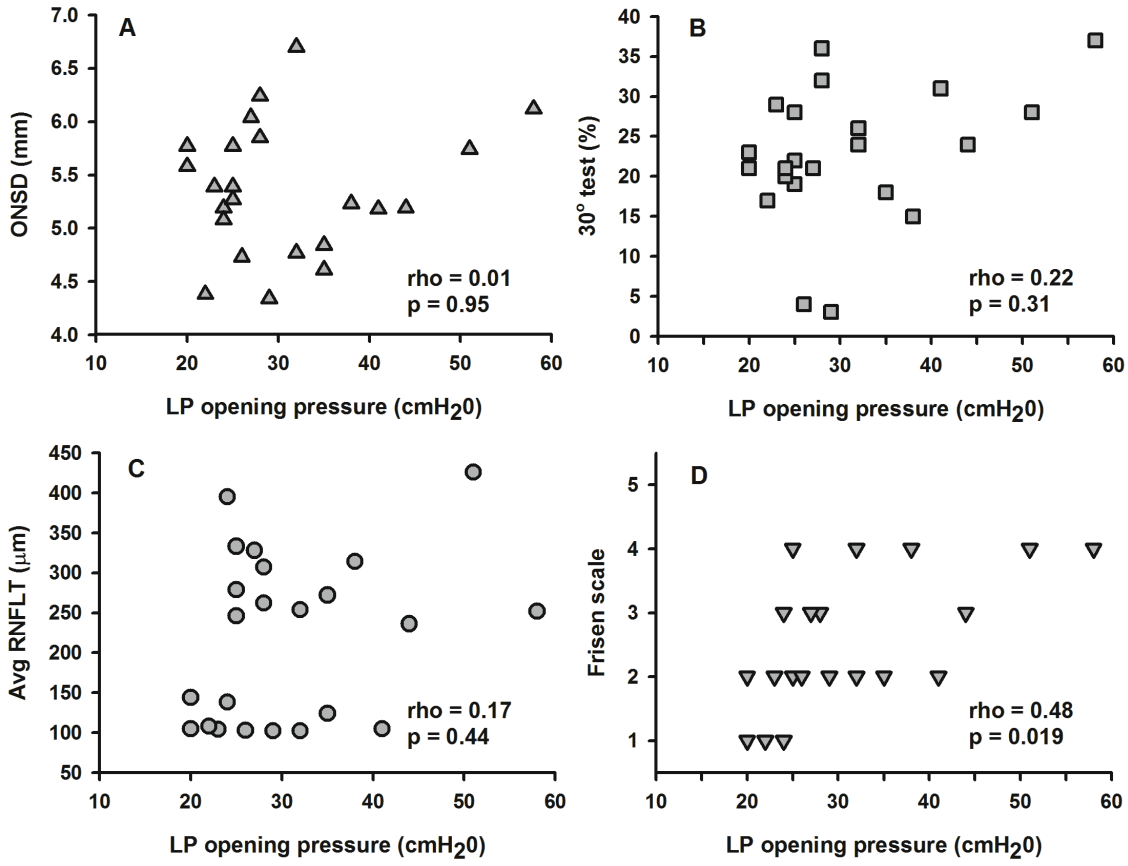

Figure 4. Scatter plot showed no observable correlation between LP opening pressure and (A) ONSD (rho = 0.01, p = 0.95), (B) 30° test (rho = 0.22, p = 0.31 B), or (C) avg RNFLT (rho = 0.17, p = 0.44, C). However, a significant correlation was seen between (D) LP opening pressure and the Frisen scale (rho = 0.48, p = 0.019, D).

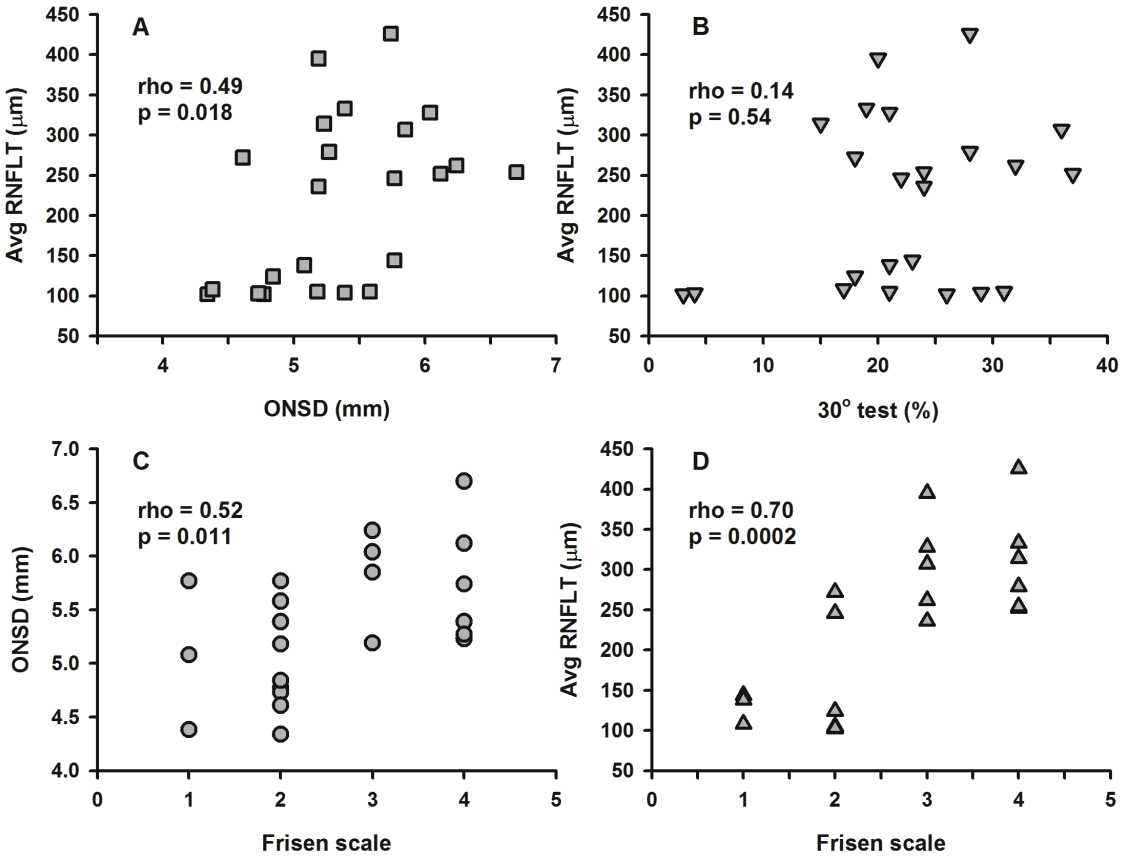

Figure 5. Scatterplots showed correlation between avg RNFLT and ONSD (A: rho = 0.49, p = 0.018), but not between avg RNFLT and 30° test (B: rho = 0.14, p = 0.54). Frisen scale grading correlated with both ONSD (C: rho = 0.52, p = 0.011) and RNFLT (D: rho = 0.70, p = 0.0002).

Interocular Asymmetry

Among the 23 patients with PE, 26.1% (n = 6) showed one grade of interocular difference in Frisen scale, and 8.7% (n = 2) showed two grades of difference. Figure 6 shows a scatter plot of ONSD (A) and avg RNFLT (B) from each eye (filled and open symbols for PE and PPE, respectively) with the solid diagonal line indicating equal values between the two eyes. Compared to PPE, the amount of interocular asymmetry

was much more noticeable for avg RNFLT than for ONSD. In Figure 6C, the interocular avg RNFLT difference was plotted against the interocular ONSD difference with dashed lines indicating zero difference in ONSD (vertical dashed line) and avg RNFLT (horizontal dashed line). Ten (43.5%) PE patients showed RNFLT difference exceeding the range of PPE patients whereas only 3 (13.0%) patients' ONSD difference exceeded the range in PPE.

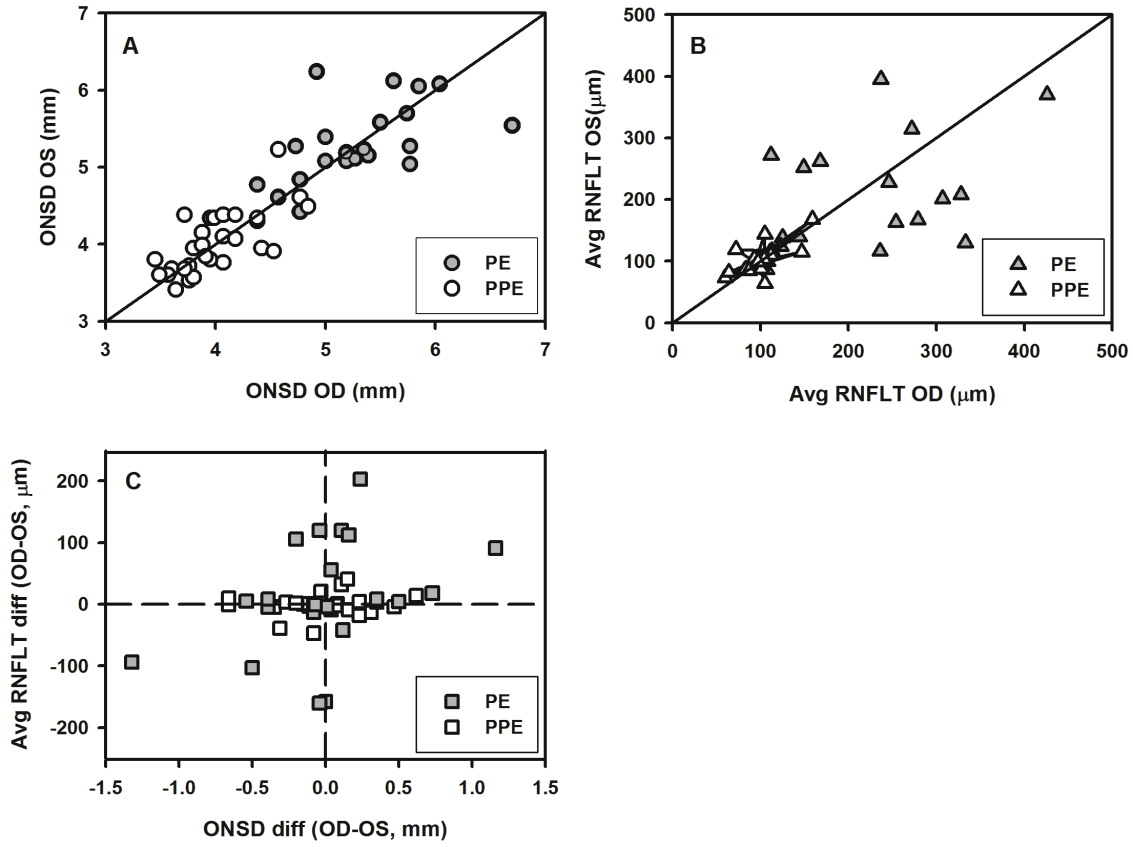

Figure 6. ONSD (A) and avg RNFLT (B) in OD was plotted against that in OS, with each data point representing an individual patient. The solid diagonal line indicates equal values between the two eyes. C. Interocular avg RNFLT difference was compared to interocular ONSD difference, with dashed lines indicating zero difference in avg RNFLT (horizontal dashed line) and ONSD (vertical dashed line). Compared to PPE (open symbols), the amount of interocular asymmetry for PE was much more noticeable for avg RNFLT than for ONSD.

Chapter 4: Discussion

Both ultrasound and OCT provided useful information for differentiating between PE and PPE in a group of patients referred to the neuro-ophthalmological service for suspected PE. However, ONSD and the 30° test showed better diagnostic abilities than OCT in distinguishing PE from PPE.

The ONSD and the 30° test in PE and PPE

The 91.3% sensitivity of ONSD and the 30° test in our study compare favorably with studies done by Carter et al (13) and Neudorfer et al (12), who found a sensitivity of 90% and 85%, respectively. Our study showed a higher specificity (96%) when compared to both studies (63-79%). To classify a positive ultrasound test, Carter et al used both the ONSD > 3.3 mm and a positive 30° test (>10% change in ONSD) and found a specificity of 79% in an adult population: whereas Neudorfer, in a pediatric population, only used ONSD > 3.3 mm and reported a specificity of 63%. For our study, if the > 10% criterion was used, the 30° test showed 91.3% sensitivity and 85.7% specificity. The difference in the study population, the severity of the PE along with the ultrasonagrapher's experience could all contribute to the difference in specificities. The optimum cut-off based on the current study cohort was > 4.59 mm for ONSD and > 13.5% for 30° test, although individual labs should have their own values established.

Of the 23 PE patients, two (9%) had normal ONSD. The first was a 35-year-old obese (BMI = 35) female who presented with headaches, tinnitus, and transient visual obscurations. Examination showed a Frisen grade II PE, 4.34 mm ONSD, a negative 30° test (3%), normal avg RNFLT, a thickened (> 95% age-matched machine norm) inferior RNFLT, and elevated LP OP (29 cm of H_20). This patient shows that in some

individuals, the CSF along the retrobulbar optic nerve sheath might be minimal despite an increased ICP. There may be restriction of CSF as it passes from the chiasmal cistern through the optic canal into the perioptic subarachnoid space. A smaller optic canal (93), whether congenital or secondary to a meningiothelial cell overgrowth (94), or a very dense network of arachnoid trabeculae and septae could be preventing the facility of CSF into the perioptic subarachnoid space (18, 95).

The second patient, a 16-year-old overweight (BMI = 27) female, presented with headaches, Frisen grade I PE, 4.38 mm ONSD, a positive 30° test (17%), normal avg RNFLT, a thickened inferior RNFLT, and a borderline lumbar puncture (22 cm of H_2O). Treatment was initiated and over the following 8 months, there was marked improvement in symptoms and optic nerve head appearance (avg RNFLT decreasing from 108 to 95 μm). There is a normal variation in ONSDs (96) and it is important for clinicians to be aware that some patients can have a lower pre-morbid ONSD. This is a case in which the 30° test, although difficult to perform, was helpful in making the correct diagnosis. These two cases demonstrate some of the limitations of orbital ultrasound and the difficulty in diagnosing accurately all PE patients. Clinicians should integrate clinical history with exam findings and order further testing if there is a strong suspicion of PE despite a negative orbital ultrasonography finding.

Of the PPE patients, only one (4%), a 12-year old male presenting with headaches, had a large ONSD (4.61mm). Examination showed large buried drusen, a negative 30° test (6%), and a thickened avg RNFLT. This rare phenomenon of PPE patients presenting with larger than normal ONSD has been reported in previous studies (12, 13). In a case report by Sadda et al, a symptomatic PPE patient with an enlarged ONSD underwent three normal lumbar punctures over an eight year period with no improvement in symptoms or optic nerve appearance (97). This could also be attributed

to a normal variation in anatomy and/or optic nerve sheath compliance (68), which means it is possible to have a relatively large ONSD despite a normal ICP. Although our study couldn't prove that the 30° test performed better than ONSD, this finding would lead one to believe that the 30° test could perform better than the ONSD in detecting PE from PPE. Nevertheless, orbital ultrasonography is a very useful test in differentiating PE from PPE; the three cases discussed above emphasize that orbital ultrasonography should not be used in isolation for diagnosing PE or PPE.

OCT in PE and PPE

Similar to our study, previous OCT studies have found an increase in the avg and quadrant RNFL thicknesses in optic disc edema compared to pseudo optic disc edema (76-79). Unlike our study where we examined only PE, most of these studies included a heterogeneous group of optic disc edema including PE, ischemic optic neuropathies, and optic neuritis and used various types of OCT machines (Table. 4) making direct comparisons difficult. Despite that, the diagnostic performance (AUC) for the RNFL thickness is similar in the current study (0.83 to 0.90) and several previous reports (0.73 to 0.87, except 0.64 at nasal quadrant in Bassi et al 2014) (11, 76, 77, 79). However, one Cirrus OCT study by Flores et al, in which the PPE group consisted of buried and surface drusen, reported higher AUC values (0.92 to 0.97), which is likely due to a relatively thin RNFL thickness in their optic drusen group (88 μm avg RNFL compared to 102 - 128 μm in other studies, Table 4) (78). RNFL thinning can be associated with optic disc drusen (98, 99); however, of the 13 optic drusen eyes in our study, only one eye showed abnormally thin avg RNFL thickness (exceeding 99% age-matched machine norms) and our mean avg RNFL thickness was 104.9 μm. Our buried drusen RNFLT measurements compared similarly with Kulkarni et al (all quadrants within 15 μm) (84),

but Lee et al, who had a larger group (n = 58) of buried drusen patients measured with SD-OCT, showed a thicker temporal RNFLT (110 μm) compared to our temporal RNFLT (66 μm) (86). Lee et al, found that larger buried drusen cause an increase in temporal RNFLT, thus one possibility is that the Lee study had larger sized buried drusen compared to our study. The average age in the Lee study was 13.5 years old compared to 26.8 years in ours. Thus, another possibility is that the buried drusen in our study, with time, are causing a focal axonal degeneration attributing to the decreased RNFLT temporally. Since buried drusen have many different presentations, in our experience, it presents as one of the most challenging situations when differentiating between PPE and PE, especially if the clinician doesn't have the equipment to perform a B-scan in office.

Table 4: Literature review of OCT RNFLT in PE and PPE

Study, Year (Ref)		Avg	S	N	I	T	OCT	Notes:
Johnson et al, 2009 (76)	mean RNFLT ODE/PPE		207/122	176/79	247/154	180/86	Stratus	20 ODE (10 PE, 5NAION, 5 ON)
	RNFLT cutoff		149	86	165	97		20 PPE (11 buried, 5 visible, 4 mix drusen)
	Sen/Spec		75/80	80/70	65/75	80/70		
	AUC		0.83	0.86	0.80	0.83		
Lee et al, 2011(77)	mean RNFLT ODE/PPE	174/119		100/53		151/107	Spectralis	15 ODE (4 NAION, 4 uveitic, 4 PE, 1 ON,
	RNFLT cutoff			78				1 CRVO, 1 diabetic)
	Sen/Spec			80/89				45 PPE (45 buried drusen)
	AUC			0.866				
Flores et al, 2012 (78)	mean RNFLT ODE/PPE	202/88	261/100	174/66	262/113	135/71	Cirrus	31 ODE (16 PE, 9 ION, 3 ON, 2 CRVO,
	RNFLT cutoff	115	159	91	158	88		1 HO)
	Sen/Spec	91/97	94/90	88/94	91/81	86/71		66 PPE (38 visible & 28 buried drusen)
	AUC	0.97	0.96	0.96	0.92	0.97		
Sarac et al, 2012 (79)	mean RNFLT ODE/PPE	157/128		133/87		133/102	RTVue	25 ODE (11 PE, 8NAION, 6 ON)
	RNFLT cutoff			74.5		101.5		25 PPE (25pts unspecified drusen)
	Sen/Spec			92/47		92/65		
	AUC			0.85		0.82		
Vartin et al, 2012 (83)	mean RNFLT PE	122	145	88	149	69	Cirrus	18 PE (Fr I and II only)
Lee et al, 2013 (86)	mean RNFLT PPE	119		54		110	Spectralis	58 PPE (58 buried drusen)

Bassi and Mohana, 2014 (11)	mean RNFLT PE/PPE	185/122	226/167	162/101	265/153	90/75	Cirrus	30 PE (15pts)
	RNFLT cutoff	133.5	170.57	113.5	172.5	77.5		31 PPE (11 unspecified drusen.
	Sen/Spec	70/65	7/65	73/71	70/61	63/55		20 unspecified PPE)
	AUC	0.78	0.768	0.79	0.73	0.64		
Kulkarni et al, 2014 (84)	mean RNFLT PE/PPE		178/137	132/77	206/140	83/77	Cirrus/ Spectralis	16 PE (9 patients – Fr I and II only) 12 PPE (6 patients)
Saenz et al, 2016	mean RNFLT PE/PPE	219/102	278/123	173/80	281/137	121/66	Cirrus	23 PE
	RNFLT cutoff	104.5	152.5	83.5	152.5	73.5		28 PPE (13 buried drusen, 15 nasally elevated)
	Sen/Spec	83/61	70/93	74/82	83/79	78/82		
	AUC	0.87	0.83	0.83	0.90	0.84		

PE: papilledema; PPE: pseudopapilledema; Avg, S, N, I, T: average, superior, nasal, inferior, temporal quadrant RNFLT; OCT: optical coherence tomography; Sens/Spec: Sensitivity/Specificity; AUC: area under the ROC curve; ODE: optic disc edema; NAION: non-arteritic ischemic optic neuropathy; ON: optic neuritis; CRVO: central retinal vein occlusion; ION: ischemic optic neuropathy; HO: hypotony; Fr: Frisen grading scale.

Some authors have suggested that the RNFL thickening in the nasal quadrant has the greatest diagnostic value (76, 77, 79); however, our data did not show a statistically significant difference in the AUCs among various quadrants. In our study, the AUC was the highest (0.90) for the inferior quadrant RNFL; supporting Dr. Hayreh's observation that "optic disc edema in raised intracranial pressure first appeared at the lower pole" in the monkey model (18). Dr. Hayreh proposed that the regions with thicker fibers in normal eyes such as the inferior quadrant (100) are more prone to axoplasmic flow stasis, resulting in early optic disc edema.

Ultrasound and OCT in differentiating mild PE (Frisen I and II) from PPE

In our study, both ultrasound (ONSD or 30° test) and OCT (avg or quadrant RNFLT) correctly diagnosed all PE eyes with Frisen scale III and IV. However, we recognize that the real diagnostic challenge for eye care providers lies in differentiating between mild PE and PPE. We did additional analysis (Table 5) by comparing the 15 PE eyes with Frisen scale I and II (if both eyes of an individual meet the criteria, the eye with lower RNFLT was chosen) to the PPE group (in each individual, the eye with higher RNFLT was chosen). Compared to all PE eyes included, the ultrasound showed slightly reduced AUC and sensitivity (at 96.4% specificity): 0.95 AUC and 80% sensitivity for the ONSD, 0.93 and 86.7% for the 30° test (Figure 3B and Table 5). For RNFLT, the AUC decreased to 0.61 - 0.77; sensitivity at 96.4% specificity ranged from 6.7% to 13.3%, showing very poor performance. Recently a small study by Kulkarni et al included 9 mild PE and 6 PPE patients and showed no difference in RNFLT between the two groups (84), but our study showed a statistical difference in the mean values (Table 5) of avg, superior, and inferior RNFLT in mild PE compared to the respective values in the PPE group.

Table 5: Diagnostic performance for ultrasound and OCT in differentiating mild PE (Fr I-II) from PPE

	Mean Values for Mild PE (n=15)	AUC (95% CI)	Cutoff value	Sensitivity%* (95% CI)
ONSD	4.97±0.43 mm	0.95 (0.89-1.02)	4.59 mm	80.0 (51.9-95.7)
30^{o} test	20.13±9.26%	0.93 (0.84-1.03)	13.50%	86.7 (59.5-98.4)
Avg RNFLT	121.6±33.76 μm	0.71 (0.55-0.87)	146.5 μm	13.3 (16.6-40.5)
S	150.53±56.47 μm	0.64 (0.44-0.83)	154.0 μm	40.0 (16.3-67.7)
N	105.80±51.96 μm	0.77 (0.62-0.93)	202.0 μm	6.7 (0.2-32.0)
I	159.87±40.97 μm	0.70 (0.54-0.86)	213.5 μm	6.7 (0.2-32.0)
T	70.47±15.55 μm	0.61 (0.43-0.79)	105.5 μm	6.7 (0.2-32.0)

*For all measurements, specificity (95% CI) was set to 96.4% (81.7%-99.9%).

Fr I-II: Frisen scale I-II; PE: papilledema; PPE: pseudopapilledema; AUC: area under the curve; S, N, I, T: superior, nasal, inferior, and temporal quadrant RNFL thickness.

Considering the disease mechanism of PE and PPE, it is not surprising that the ultrasound performed much better than OCT in differentiating mild PE from PPE. In PE, the elevated ICP is first transmitted to the perioptic subarachnoid space, causing an increase in ONSD, which then cause axoplasmic flow stasis and subsequent swelling of the RNFL (18). In some eyes with good optic nerve sheath compliance, when the perioptic CSF pressure is mild to moderate, the sheath expansion might balance out some of the pressure rise, leading to only mild axonal swelling anteriorly. In PPE, the anatomical changes occur anteriorly in the optic disc (drusen lie anteriorly to lamina cribrosa affecting OCT measurements) (35), not affecting the retrobulbar optic nerve sheath.

Retinal ganglion cell integrity in PE and PPE

As GCIPT is a sensitive measurement in glaucoma (101) and multiple sclerosis (102); we also examined GCIPT in PE for potential ganglion cell loss. The GCIP layer proved to have no diagnostic value, and was neither increased nor decreased in PE. It is worth mentioning that the GCIPT at the initial visit in 26% PE patients (n = 6/23) were flagged as “red” (below 99% of the machine normative values) that was due to inaccurate segmentation, despite great signal strength. Once the PE had resolved, which occurred in all patients, the GCIPT returned to “normal” when compared to age matched norms. Clinicians and researchers should take caution when reporting and monitoring these values.

Relationship between various measurements in PE

In our study, Frisen scale was moderately correlated with LP opening pressure (Spearman rho = 0.48), ONSD (rho = 0.52) and avg RNFLT (rho = 0.70), suggesting a general trend of more severe PE in those with higher LP opening pressure. However, a correlation between LP opening pressure and ONSD or RNFLT was not observed. The lack of a correlation could be attributed to the fact that ocular measurements and LP were not performed at the same time. However, the concept of uniformly distributed CSF pressure in patients with PE is challenged by the presence of asymmetric and unilateral PE (see section below), absence of PE in some patients with raised ICP (103), and the persistence of PE in some with normalized ICP (104). Killer et al proposed the idea of "compartment" of the perioptic subarachnoid spaces, as evidenced by the markedly different CSF protein concentrations in the lumbar CSF and perioptic CSF in patients with PE (105), and reduced perioptic CSF flow compared to that in suprasellar cistern in some IIH patients (106). In other words, the perioptic CSF pressure causing PE is not necessarily expected to be equal to that of LP opening pressure; therefore, a nice correlation between LP opening pressure and ONSD or RNFLT may not exist.

Asymmetry in PE

Previous studies reported that 4 - 7.5% of PE patients exhibit very asymmetric PE (defined as ≥ 2 Frisen scale difference) (54, 93). In our study, 2 (8.7%) PE patients met the criterion of severe asymmetry (grade II Frisen scale in one eye and IV in contralateral eye). The mechanism underlying the asymmetry is unsettled. Lepore (1992) proposed the role of bilateral differences in collagen thickness and elasticity at the lamina cribrosa or the optic nerve sheath (4), while others (93, 104) suggested optic canal anatomy as a contributing factor. Based on brain imaging of those with very asymmetric PE, Bidot et al (2014) found smaller optic canals on the side with less optic

disc edema in all (8 out of 8) and less perioptic nerve CSF in 50% (6 of 12) of the subjects (93). They believed that the smaller optic canal restricts the amount of CSF transmitted to the perioptic subarachnoid space, resulting in less disc edema. It is unclear if the smaller optic canal is congenital or acquired, for example, meningiothelial cells may play a role since they proliferate in response to elevated ICP (94) and could potentially decrease the optic canal size to variable degrees between the eyes. Interestingly, 43.5% (10/23) of our patients showed RNFL asymmetry exceeding the difference in control (PPE), however, only 8.7% (2/23) patients had ONSD difference larger than the range in control. The two patients with very asymmetric PE showed 8.5% and 4.7% interocular difference in ONSD (difference/mean size) compared to 51.4% and 43.8% RNFLT difference. Our data is in agreement with the report by Huna-Baron et al (2001) where neuroimaging in 15 patients with unilateral PE did not show a gross difference (none larger than 0.5 mm) in ONSD (107), supporting that factors such as difference in lamina cribrosa might play a role. However, our finding doesn't necessarily contradict the hypothesis of asymmetrical preoptic pressure secondary to different optic canal sizes. It is plausible that after the optic nerve sheath distension reaches its limit bilaterally (68), the side with higher perioptic CSF pressure would lead to greater disc swelling. It is also possible that the ultrasound is not as sensitive as OCT in detecting interocular differences. Further research may shed light into this topic, which has particular interest in astronauts, where it has been reported that 4 of 7 astronauts had asymmetric PE, all worse in the right eye (108).

Limitations of current study and future direction

The limitations of the present study include the retrospective nature, relatively small sample size, potential sampling bias, and the physician being unmasked to ultrasound and OCT results. Since this study was done with patients from a tertiary neuro-ophthalmologist, our results were skewed towards cases with difficult diagnostic decisions, especially in the PPE group. Compared to Carter et al, where 67% of PPE patients were asymptomatic (13), every PPE patient presented with at least one symptom (HA, TVO, tinnitus), which is what warranted the referral. Our neuro-ophthalmologist is fully aware that IIH can occur without PE (103), therefore, careful analysis of clinical history, symptomology, when necessary communication with their neurologists or internists, and observation over time were conducted to minimize the number of false negatives.

Even though orbital ultrasound was superior to SD-OCT in differentiating PE and PPE, very few eye care providers have access to a highly trained ultrasonagrapher who can perform the standardized A scan; therefore, we are currently investigating whether same results are achievable using B scan, a much easier and faster technique to measure ONSD (66). Two recent meta-analysis have shown that in neuro-intensive units, it can accurately diagnose PE compared to normal controls with good sensitivity (90-96%) and specificity (85-92%) (65, 109). These studies do report different ONSD thresholds and thus internal validation should be considered before implementing B-scan in the diagnosis of elevated ICP (64).

Chapter 5: Conclusion

The purpose of this thesis was to evaluate the use of two non-invasive and low-cost tests, orbital ultrasound and optical coherence tomography, in differentiating papilledema (PE) from pseudopapilledema (PPE).

Accurately differentiating PE from PPE is critical because PE indicates potentially life-threatening conditions requiring urgent medical management whereas PPE is a benign condition. Making a decision based on ophthalmoscopy alone can be difficult because optic discs in PE and PPE could both appear elevated, crowded, and have indistinct margins. Knowledge gained from this research will aid clinicians in correctly diagnosing PE especially mild PE, which will facilitate early detection and treatment of ocular or systemic health conditions.

Previous studies have examined the role of optical coherence tomography (OCT) or ultrasound individually in differentiating PE and PPE; however, to our knowledge, this was the first study to include both SD-OCT and standardized A-scan in the same group of patients. If we can improve diagnostic accuracy based on objective, low-cost, non-invasive, clinically available devices such as OCT and orbital ultrasound, we will decrease or completely avoid expensive, invasive, unnecessary testing, and patient/doctor anxiety.

The main findings of this thesis are as follows:

- Since all of our patients were diagnosed with IIH, most of the patients in the PE subgroup were females of childbearing age. The most common symptom was headache, followed by TVO and tinnitus; symptoms showed no statistical difference in differentiating between PE and PPE. However, such finding may not apply to a general clinic. A high prevalence of symptoms in our PPE group is likely a reflection

of these patients being referred to a tertiary neuro-ophthalmology clinic.

- Mean ONSD and avg RNFLT measurements were greater in PE than PPE. A greater reduction on the 30° test was seen in PE compared to PPE
- Of all the orbital ultrasound and OCT measurements, ONSD and the 30° test showed the greatest diagnostic capabilities followed by the inferior RNFLT and avg RNFLT.
- In several PE patients, OCT showed GCIPT thinning on the initial visit; however, once the PE had resolved, which occurred in all patients, the GCIPT returned to "normal" when compared to age matched norms. Clinicians and researchers should take caution in interpreting this inaccurate segmentation as atrophy when reporting and monitoring these values.
- Our study supports orbital ultrasonography and SD-OCT as useful ancillary tests that can be done, along with a thorough examination, in order to effectively differentiate between PE and PPE. Due to its easy access, OCT scan of RNFL thickness can be potentially used to detect moderate to severe papilledema in a non-ophthalmologic setting. Ultrasound measurements may further assist eye care providers in differentiating mild PE from PPE when ophthalmoscopic findings are non-diagnostic.
- A future, prospective trial is needed to confirm the diagnostic abilities of OCT and orbital ultrasonography in differentiating PE from PPE.

Chapter 6: References

1. Walsh F, Hoyt, WF, Miller, NR. Walsh and Hoyt's clinical neuro-ophthalmology: the essentials. 2nd ed. Philadelphia, PA: Lippincott Williams & Wilkins; 2008.
2. Hayreh SS. Optic disc edema in raised intracranial pressure. V. Pathogenesis. Arch Ophthalmol. 1977;95(9):1553-65.
3. Tso MO, Hayreh SS. Optic disc edema in raised intracranial pressure. III. A pathologic study of experimental papilledema. Arch Ophthalmol. 1977;95(8):1448-57.
4. Lepore FE. Unilateral and highly asymmetric papilledema in pseudotumor cerebri. Neurology. 1992;42(3 Pt 1):676-8.
5. Soler D, Cox T, Bullock P, Calver DM, Robinson RO. Diagnosis and management of benign intracranial hypertension. Arch Dis Child. 1998;78(1):89-94.
6. Corbett JJ, Savino PJ, Thompson HS, Kansu T, Schatz NJ, Orr LS, et al. Visual loss in pseudotumor cerebri. Follow-up of 57 patients from five to 41 years and a profile of 14 patients with permanent severe visual loss. Arch Neurol. 1982;39(8):461-74.
7. Carta A, Favilla S, Prato M, Bianchi-Marzoli S, Sadun AA, Mora P. Accuracy of funduscopy to identify true edema versus pseudoedema of the optic disc. Invest Ophthalmol Vis Sci. 2012;53(1):1-6.
8. Duncan JE, Freedman SF, El-Dairi MA. The incidence of neovascular membranes and visual field defects from optic nerve head drusen in children. J AAPOS. 2016;20(1):44-8.
9. Malmqvist L, Wegener M, Sander BA, Hamann S. Peripapillary Retinal Nerve Fiber Layer Thickness Corresponds to Drusen Location and Extent of Visual Field Defects in Superficial and Buried Optic Disc Drusen. J Neuroophthalmol. 2016;36(1):41-5.
10. Friedman DI, Liu GT, Digre KB. Revised diagnostic criteria for the pseudotumor cerebri syndrome in adults and children. Neurology. 2013;81(13):1159-65.
11. Bassi ST, Mohana KP. Optical coherence tomography in papilledema and pseudopapilledema with and without optic nerve head drusen. Indian J Ophthalmol. 2014;62(12):1146-51.
12. Neudorfer M, Ben-Haim MS, Leibovitch I, Kesler A. The efficacy of optic nerve ultrasonography for differentiating papilloedema from pseudopapilloedema in eyes with swollen optic discs. Acta Ophthalmol.91(4):376-80.
13. Carter SB, Pistilli M, Livingston KG, Gold DR, Volpe NJ, Shindler KS, et al. The role of orbital ultrasonography in distinguishing papilledema from pseudopapilledema. Eye (Lond). 2014;28(12):1425-30.
14. Pineles SL, Arnold AC. Fluorescein angiographic identification of optic disc drusen with and without optic disc edema. J Neuroophthalmol. 2012;32(1):17-22.
15. Türck L. Ein Fall von Hämorrhagie der Netzhaut beider Augen. Zeit Ges Wien Ärzte. 1853;9(1):214-8.
16. von Graefe A. Sur certaines altérations de la rétine et du nerf optique, en rapport avec des affections cérébales. Gaz Herdom. 1860;7:707-8.

17. Deyl J. Choked Disk and its sequelae. System of Diseases of the Eye' Ed by WF Norris and CA Oliver. 1898;3:592-610.
18. Hayreh SS. Pathogenesis of optic disc edema in raised intracranial pressure. Prog Retin Eye Res. 2016;50:108-44.
19. Hayreh SS. Pathogenesis of Oedema of the Optic Disc (papilloedema): University College London (University of London); 1965.
20. Hayreh SS. Occlusion of the central retinal vessels. British J of Ophthalmol. 1965;49(12):626.
21. Hayreh SS. Optic disc edema in raised intracranial pressure. VI. Associated visual disturbances and their pathogenesis. Arch Ophthalmol. 1977;95(9):1566-79.
22. Tso MO, Hayreh SS. Optic disc edema in raised intracranial pressure. IV. Axoplasmic transport in experimental papilledema. Arch Ophthalmol. 1977;95(8):1458-62.
23. Frisen L. Swelling of the optic nerve head: a staging scheme. J Neurol Neurosurg Psychiatry. 1982;45(1):13-8.
24. Scott CJ, Kardon RH, Lee AG, Frisen L, Wall M. Diagnosis and grading of papilledema in patients with raised intracranial pressure using optical coherence tomography vs clinical expert assessment using a clinical staging scale. Arch Ophthalmol. 2010;128(6):705-11.
25. Witmer MT, Margo CE, Drucker M. Tilted optic disks. Surv Ophthalmol. 2010;55(5):403-28.
26. Apple DJ, Rabb MF, Walsh PM. Congenital anomalies of the optic disc. Surv Ophthalmol. 1982;27(1):3-41.
27. Brito PN, Vieira MP, Falcao MS, Faria OS, Falcao-Reis F. Optical coherence tomography study of peripapillary retinal nerve fiber layer and choroidal thickness in eyes with tilted optic disc. J Glaucoma. 2015;24(1):45-50.
28. Vongphanit J, Mitchell P, Wang JJ. Population prevalence of tilted optic disks and the relationship of this sign to refractive error. Am J Ophthalmol. 2002;133(5):679-85.
29. Oliveira C, Harizman N, Girkin CA, Xie A, Tello C, Liebmann JM, et al. Axial length and optic disc size in normal eyes. British J of Ophthalmol. 2007;91(1):37-9.
30. Jonas JB, Gusek GC, Guggenmoos-Holzmann I, Naumann GO. Pseudopapilledema associated with abnormally small optic discs. Acta Ophthalmol. 1988;66(2):190-3.
31. Jonas JB, Gusek GC, Naumann GO. Optic disc, cup and neuroretinal rim size, configuration and correlations in normal eyes. Invest Ophthalmol Vis Sci. 1988;29(7):1151-8.
32. Straatsma BR, Foos RY, Heckenlively JR, Taylor GN. Myelinated retinal nerve fibers. Am J Ophthalmol. 1981;91(1):25-38.
33. Lorentzen SE. Drusen of the optic disk. A clinical and genetic study. Acta Ophthalmol. 1966:Suppl 90: 1.
34. Friedman AH, Beckerman B, Gold DH, Walsh JB, Gartner S. Drusen of the optic disc. Surv Ophthalmol. 1977;21(5):373-90.

35. SAMUELS B. Drusen of the optic papilla: A clinical and pathologic study. Arch Ophthalmol. 1941;25(3):412-23.

36. Erkkilä H. Optic disc drusen in children. Acta Ophthalmol Supplementum. 1976(129):3-44.

37. Tso MO. Pathology and pathogenesis of drusen of the optic nervehead. Ophthalmology. 1981;88(10):1066-80.

38. Auw-Haedrich C, Staubach F, Witschel H. Optic disk drusen. Surv Ophthalmol. 2002;47(6):515-32.

39. Sacks JG, O'Grady RB, Choromokos E, Leestma J. The pathogenesis of optic nerve drusen. A hypothesis. Arch Ophthalmol. 1977;95(3):425-8.

40. Mullie MA, Sanders MD. Computed tomographic diagnosis of buried drusen of the optic nerve head. Can J Ophthalmol. 1985;20(3):114-7.

41. Floyd MS, Katz BJ, Digre KB. Measurement of the scleral canal using optical coherence tomography in patients with optic nerve drusen. Am J Ophthalmol. 2005;139(4):664-9.

42. Boldt HC, Byrne SF, DiBernardo C. Echographic evaluation of optic disc drusen. J Clin Neuroophthalmol. 1991;11(2):85-91.

43. Kiegler HR. [Comparison of functional findings with results of standardized echography of the optic nerve in optic disk drusen]. Wien Klin Wochenschr. 1995;107(21):651-3.

44. Lorentzen SE. Drusen of the optic disk, an irregularly dominant hereditary affection. Acta Ophthalmol (Copenh). 1961;39:626-43.

45. Spencer TS, Katz BJ, Weber SW, Digre KB. Progression from anomalous optic discs to visible optic disc drusen. J Neuroophthalmol. 2004;24(4):297-8.

46. Mustonen E. Pseudopapilloedema with and without verified optic disc drusen. A clinical analysis II: visual fields. Acta Ophthalmol (Copenh). 1983;61(6):1057-66.

47. Savino PJ, Glaser JS, Rosenberg MA. A clinical analysis of pseudopapilledema. II. Visual field defects. Arch Ophthalmol. 1979;97(1):71-5.

48. Beck RW, Corbett JJ, Thompson HS, Sergott RC. Decreased visual acuity from optic disc drusen. Arch Ophthalmol. 1985;103(8):1155-9.

49. Hoover DL, Robb RM, Petersen RA. Optic disc drusen in children. J Pediatr Ophthalmol Strabismus. 1988;25(4):191-5.

50. Lee AG, Zimmerman MB. The rate of visual field loss in optic nerve head drusen. Am J Ophthalmol. 2005;139(6):1062-6.

51. Lam BL, Morais CG, Jr., Pasol J. Drusen of the optic disc. Curr Neurol Neurosci Rep. 2008;8(5):404-8.

52. Durcan FJ, Corbett JJ, Wall M. The incidence of pseudotumor cerebri. Population studies in Iowa and Louisiana. Arch Neurol. 1988;45(8):875-7.

53. Giuseffi V, Wall M, Siegel PZ, Rojas PB. Symptoms and disease associations in idiopathic intracranial hypertension (pseudotumor cerebri): a case-control study. Neurology. 1991;41(2 (Pt 1)):239-44.

54. Wall M, Kupersmith MJ, Kieburtz KD, Corbett JJ, Feldon SE, Friedman DI, et al. The idiopathic intracranial hypertension treatment trial: clinical profile at baseline. JAMA Neurol. 2014;71(6):693-701.

55. Wall M, George D. Idiopathic intracranial hypertension. A prospective study of 50 patients. Brain. 1991;114 (Pt 1A):155-80.

56. Bono F, Messina D, Giliberto C, Cristiano D, Broussard G, D'Asero S, et al. Bilateral transverse sinus stenosis and idiopathic intracranial hypertension without papilledema in chronic tension-type headache. J Neurol. 2008;255(6):807-12.

57. Bono F, Messina D, Giliberto C, Cristiano D, Broussard G, Fera F, et al. Bilateral transverse sinus stenosis predicts IIH without papilledema in patients with migraine. Neurology. 2006;67(3):419-23.

58. Mathew NT, Ravishankar K, Sanin LC. Coexistence of migraine and idiopathic intracranial hypertension without papilledema. Neurology. 1996;46(5):1226-30.

59. Wang SJ, Silberstein SD, Patterson S, Young WB. Idiopathic intracranial hypertension without papilledema: a case-control study in a headache center. Neurology. 1998;51(1):245-9.

60. Kovarik JJ, Doshi PN, Collinge JE, Plager DA. Outcome of pediatric patients referred for papilledema. J AAPOS. 2015;19(4):344-8.

61. Sadun AA, Currie JN, Lessell S. Transient visual obscurations with elevated optic discs. Ann Neurol. 1984;16(4):489-94.

62. Hofmann E, Behr R, Neumann-Haefelin T, Schwager K. Pulsatile tinnitus: imaging and differential diagnosis. Dtsch Arztebl Int. 2013;110(26):451-8.

63. Wall M. Idiopathic intracranial hypertension. Neurol Clin. 2010;28(3):593-617.

64. Rajajee V, Vanaman M, Fletcher JJ, Jacobs TL. Optic nerve ultrasound for the detection of raised intracranial pressure. Neurocrit Care.15(3):506-15.

65. Dubourg J, Javouhey E, Geeraerts T, Messerer M, Kassai B. Ultrasonography of optic nerve sheath diameter for detection of raised intracranial pressure: a systematic review and meta-analysis. Intensive Care Med.37(7):1059-68.

66. Bauerle J, Schuchardt F, Schroeder L, Egger K, Weigel M, Harloff A. Reproducibility and accuracy of optic nerve sheath diameter assessment using ultrasound compared to magnetic resonance imaging. BMC Neurol.13:187.

67. Helmke K, Hansen HC. Fundamentals of transorbital sonographic evaluation of optic nerve sheath expansion under intracranial hypertension. I. Experimental study. Pediatr Radiol. 1996;26(10):701-5.

68. Hansen HC, Helmke K. Validation of the optic nerve sheath response to changing cerebrospinal fluid pressure: ultrasound findings during intrathecal infusion tests. J Neurosurg. 1997;87(1):34-40.

69. Ossoinig KC. Standardized echography: basic principles, clinical applications, and results. Int Ophthalmol Clin. 1979;19(4):127-210.

70. Ossoinig KC, Cennamo G, Frazier-Byrne S. Echographic Differential Diagnosis of Optic-Nerve Lesions. In: Thijssen JM, Verbeek AM, editors. Ultrasonography in Ophthalmology: Proceedings of the 8th SIDUO Congress. Dordrecht: Springer Netherlands; 1981. p. 327-32.

71. Atta HR. Imaging of the optic nerve with standardised echography. Eye (Lond). 1988;2 (Pt 4):358-66.

72. Bryne SF GR. Ultrasound of the eye and orbit. St Louis (MO): Mosby; 2002.

73. Frisen L, Scholdstrom G, Svendsen P. Drusen in the optic nerve head. Verification by computerized tomography. Arch Ophthalmol. 1978;96(9):1611-4.

74. Kelley JS. Autofluorescence of drusen of the optic nerve head. Arch Ophthalmol. 1974;92(3):263-4.

75. Kurz-Levin MM, Landau K. A comparison of imaging techniques for diagnosing drusen of the optic nerve head. Arch Ophthalmol. 1999;117(8):1045-9.

76. Johnson LN, Diehl ML, Hamm CW, Sommerville DN, Petroski GF. Differentiating optic disc edema from optic nerve head drusen on optical coherence tomography. Arch Ophthalmol. 2009;127(1):45-9.

77. Lee KM, Woo SJ, Hwang JM. Differentiation of optic nerve head drusen and optic disc edema with spectral-domain optical coherence tomography. Ophthalmology. 2011;118(5):971-7.

78. Flores-Rodriguez P, Gili P, Martin-Rios MD. Sensitivity and specificity of time-domain and spectral-domain optical coherence tomography in differentiating optic nerve head drusen and optic disc oedema. Ophthalmic Physiol Opt. 2012;32(3):213-21.

79. Sarac O, Tasci YY, Gurdal C, Can I. Differentiation of optic disc edema from optic nerve head drusen with spectral-domain optical coherence tomography. J Neuroophthalmol. 2012;32(3):207-11.

80. Hedges TR, 3rd, Legge RH, Peli E, Yardley CJ. Retinal nerve fiber layer changes and visual field loss in idiopathic intracranial hypertension. Ophthalmology. 1995;102(8):1242-7.

81. Kupersmith MJ, Sibony P, Mandel G, Durbin M, Kardon RH. Optical coherence tomography of the swollen optic nerve head: deformation of the peripapillary retinal pigment epithelium layer in papilledema. Invest Ophthalmol Vis Sci. 2011;52(9):6558-64.

82. Skau M, Milea D, Sander B, Wegener M, Jensen R. OCT for optic disc evaluation in idiopathic intracranial hypertension. Graefes Arch Clin Exp Ophthalmol. 2011;249(5):723-30.

83. Vartin CV, Nguyen AM, Balmitgere T, Bernard M, Tilikete C, Vighetto A. Detection of mild papilloedema using spectral domain optical coherence tomography. Br J Ophthalmol. 2012;96(3):375-9.

84. Kulkarni KM, Pasol J, Rosa PR, Lam BL. Differentiating mild papilledema and buried optic nerve head drusen using spectral domain optical coherence tomography. Ophthalmology.121(4):959-63.

85. Savini G, Bellusci C, Carbonelli M, Zanini M, Carelli V, Sadun AA, et al. Detection and quantification of retinal nerve fiber layer thickness in optic disc edema using stratus OCT. Arch Ophthalmol. 2006;124(8):1111-7.

86. Lee KM, Woo SJ, Hwang JM. Morphologic characteristics of optic nerve head drusen on spectral-domain optical coherence tomography. Am J Ophthalmol. 2013;155(6):1139-47 e1.

87. Slotnick S, Sherman J. Buried disc drusen have hypo-reflective appearance on SD-OCT. Optom Vis Sci. 2012;89(5):E704-8.

88. Sato T, Mrejen S, Spaide RF. Multimodal imaging of optic disc drusen. Am J Ophthalmol. 2013;156(2):275-82 e1.

89. Merchant KY, Su D, Park SC, Qayum S, Banik R, Liebmann JM, et al. Enhanced depth imaging optical coherence tomography of optic nerve head drusen. Ophthalmology. 2013;120(7):1409-14.

90. Silverman AL, Tatham AJ, Medeiros FA, Weinreb RN. Assessment of optic nerve head drusen using enhanced depth imaging and swept source optical coherence tomography. J Neuroophthalmol. 2014;34(2):198-205.

91. Karam E, Hedges T. Optical coherence tomography of the retinal nerve fibre layer in mild papilloedema and pseudopapilloedema. Br J Ophthalmol. 2005;89(3):294-8.

92. Mwanza JC, Oakley JD, Budenz DL, Anderson DR, Cirrus Optical Coherence Tomography Normative Database Study G. Ability of cirrus HD-OCT optic nerve head parameters to discriminate normal from glaucomatous eyes. Ophthalmology. 2011;118(2):241-8 e1.

93. Bidot S, Clough L, Saindane AM, Newman NJ, Biousse V, Bruce BB. The Optic Canal Size Is Associated With the Severity of Papilledema and Poor Visual Function in Idiopathic Intracranial Hypertension. J Neuroophthalmol. 2015.

94. Xin X, Fan B, Flammer J, Miller NR, Jaggi GP, Killer HE, et al. Meningothelial cells react to elevated pressure and oxidative stress. PLoS One. 2011;6(5):e20142.

95. Killer HE, Laeng HR, Flammer J, Groscurth P. Architecture of arachnoid trabeculae, pillars, and septa in the subarachnoid space of the human optic nerve: anatomy and clinical considerations. Br J Ophthalmol. 2003;87(6):777-81.

96. Hansen HC, Helmke K, Kunze K. Optic Nerve Sheath Enlargement in Acute Intracranial Hypertension. Neuro-Ophthalmol. 1994;14(6):345-54.

97. Sadda SR, DiBernardo C, Miller NR. Anomalous optic disc elevation associated with ultrasonographic evidence of increased subarachnoid fluid. J Neuroophthalmol. 2000;20(1):25-7.

98. Katz BJ, Pomeranz HD. Visual field defects and retinal nerve fiber layer defects in eyes with buried optic nerve drusen. Am J Ophthalmol. 2006;141(2):248-53.

99. Roh S, Noecker RJ, Schuman JS, Hedges TR, 3rd, Weiter JJ, Mattox C. Effect of optic nerve head drusen on nerve fiber layer thickness. Ophthalmol. 1998;105(5):878-85.

100. Alasil T, Wang K, Keane PA, Lee H, Baniasadi N, de Boer JF, et al. Analysis of normal retinal nerve fiber layer thickness by age, sex, and race using spectral domain optical coherence tomography. J Glaucoma. 2013;22(7):532-41.

101. Hood DC, Raza AS, de Moraes CG, Liebmann JM, Ritch R. Glaucomatous damage of the macula. Prog Retin Eye Res. 2013;32:1-21.

102. Narayanan D, Cheng H, Bonem KN, Saenz R, Tang RA, Frishman LJ. Tracking changes over time in retinal nerve fiber layer and ganglion cell-inner plexiform layer thickness in multiple sclerosis. Mult Scler. 2014;20(10):1331-41.

103. Aylward SC, Aronowitz C, Roach ES. Intracranial Hypertension Without Papilledema in Children. J Child Neurol. 2016;31(2):177-83.

104. Killer HE, Subramanian PS. Compartmentalized cerebrospinal fluid. Int Ophthalmol Clin. 2014;54(1):95-102.

105. Killer HE, Jaggi GP, Flammer J, Miller NR, Huber AR. The optic nerve: a new window into cerebrospinal fluid composition? Brain. 2006;129(Pt 4):1027-30.

106. Killer HE, Jaggi GP, Flammer J, Miller NR, Huber AR, Mironov A. Cerebrospinal fluid dynamics between the intracranial and the subarachnoid space of the optic nerve. Is it always bidirectional? Brain. 2007;130(Pt 2):514-20.

107. Huna–Baron R, Landau K, Rosenberg M, Warren F, Kupersmith M. Unilateral swollen disc due to increased intracranial pressure. Neurology. 2001;56(11):1588-90.

108. Mader TH, Gibson CR, Hart SF, Lee AG. Asymmetric Papilledema in Idiopathic Intracranial Hypertension: Comment. J Neuro-ophthalmol. 2016;36(1):111-2.

109. Ohle R, McIsaac SM, Woo MY, Perry JJ. Sonography of the Optic Nerve Sheath Diameter for Detection of Raised Intracranial Pressure Compared to Computed Tomography: A Systematic Review and Meta-analysis. J Ultrasound Med. 2015;34(7):1285-94.